OptoAssay – Light-controlled Dynamic Bioassay Using Optogenetic Switches

Nadine Urban[1,2,3], Maximillian Hörner[3], Wilfried Weber[3, *], Can Dincer[1,2, *]

[1] University of Freiburg, FIT Freiburg Centre for Interactive Materials and Bioinspired Technologies, 79110 Freiburg, Germany

[2] University of Freiburg, Department of Microsystems Engineering – IMTEK, Laboratory for Sensors, 79110 Freiburg, Germany

[3] University of Freiburg, Faculty of Biology and Signalling Research Centers BIOSS and CIBSS, 79104 Freiburg, Germany

*Correspondence to W.W. and C.D.: wilfried.weber@biologie.uni-freiburg.de (W. Weber) and dincer@imtek.de (C. Dincer)

Abstract (max. 3 sentences with 70 words)

Circumventing the limitations of current bioassays, we introduce the first light-controlled assay, the OptoAssay, towards wash- and pump-free point-of-care diagnostics. Extending the capabilities of standard bioassays with light-dependent and reversible interaction of optogenetic switches, OptoAssays enable a bi-directional movement of assay components, only by changing the wavelength of light. Combined with smartphones, OptoAssays obviate the need for external flow control systems like pumps or valves and signal readout devices.

Main

Point-of care (POC) diagnostics is the key player for fast interventions that might have critical value for patient's outcome. For this purpose, POC testing that allows for rapid diagnostics in non-laboratory settings carried out by untrained personnel has become more commonplace over the last decade. Its importance has even more deepened during the ongoing Covid19 pandemic. One of the most used POC formats are paper-based devices like lateral flow assays (LFAs), where the sample is added on a cellulose-based test stripe and transported through capillary forces along the stripe. This, however, only allows for a uni-directional sample flow which fundamentally limits the flexibility in assay design and sample processing[1,2]. On the other hand, other POC devices offering bidirectional microfluidics suffer from expensive and bulky pumps or flow control systems, also requiring an additional energy source, that complicates their on-site use[3,4].

To circumvent this restraint, we present for the first time the proof-of-concept of a light-controlled dynamic bioassay (OptoAssay). OptoAssay allows for bi-directional movement of biomolecules, enabling wash-free signal readout of bioassays. For this purpose, the biomolecules fused to a phytochrome interacting factor 6 (PIF6) can be released from and rebind to the plant photoreceptor phytochrome B (PhyB) by exposure to far-red or red light, respectively, thereby circumventing the need for external flow control devices. PhyB exhibits two distinct light absorbing conformations (**Figure 1A**): a red-light absorbing P_r (red) state with λ_{max} = 650-670 nm and a far-red light absorbing, biologically active, P_{fr} (far red) state with λ_{max} = 700-730 nm. In the active state, PhyB can bind proteins from a class called phytochrome interacting factors while in the inactive state this interaction is reversed[5,6]. Up to date, this switching behavior of the PhyB/PIF systems has been used in various applications to control, for example, gene expression[7], cell signalling[8] or to create biohybrid materials[9].

Here, we apply optogenetic switches for realizing the first light-controlled dynamic bioassay and successfully demonstrate its proof-of-principle, detecting a his-tag as analyte on a nitrocellulose substrate. Besides, we show the general versatility of the assay components on other substrates, namely agarose beads and poly(methyl methacrylate) (PMMA), employed for building POC devices.

Results

The concept of the OptoAssay consists of two distinct areas (**Figure 1B**): a smaller receiver area where the signal readout is performed, is placed in the middle of the sender area into a notch so that the areas are not directly connected. These areas are later bridged by adding sample solution to both sides so that the assay components can diffuse from one area to the other. In this work, the OptoAssay is carried out as an immunoassay using antibodies. Herein, a competitive assay format was chosen, in which a competitor and the analyte in the sample compete for binding to the detection antibody. For this purpose, the sender area (**Figure 1C**), on which the light sensitive components, i.e., PhyB, immobilized via a biotin-neutravidin (nAv) interaction on the surface is linked to PIF6 that can bind or be released to or from PhyB depending on the wavelength applied. On the other hand, antibodies directed against the molecule of interest are immobilized on the receiver area.

For the proof-of-principle assay, we use a his-tagged protein (see **Methods**) as analyte and the his-tag on PIF6 as competitor that are recognized by an anti his-tag antibody. The signal readout is performed by measuring the fluorescence intensity of the competitor complex, his-tagged PIF6, to which green fluorescent protein (GFP) is fused. For the initial OptoAssay configuration, the competitor complex is attached to PhyB on the sender area during red light exposure. The assay procedure itself comprises of two steps (**Figure 1B**): first, the competitor complex is released from PhyB through far-red light illumination. At the same time, the analyte is added. Now both the analyte and the competitor can compete for binding to the antibody immobilized on the receiver area. Second, unbound competitor complexes are re-associated to PhyB present on the sender area and thus, removed from the receiver area only by applying red light. Due to the competitive assay format, the signal measured on the receiver area is inverse proportional to the concentration of the analyte. In order to enable POC testing using the OptoAssay, a 3D printed PhotoBox that allows for illumination with red and far-red light has been built (**Figure1 D,E**)[10]. The illumination can be controlled with a smartphone that is linked via a Bluetooth module to the electronics of the PhotoBox. Images of the OptoAssay results can be then easily read out, evaluated, and further transmitted using the smartphone.

As substrate material for immobilization of assay components, we chose nitrocellulose as it is widely applied for LFA devices due to its non-specific affinity to proteins[11,12]. We first investigated an appropriate blocking method for nitrocellulose to cover unoccupied spaces after the protein of interest has been immobilized. Therefore, we examined the blocking performance of bovine serum albumin (BSA) and casein. The results (**Figure S1**) suggest that albeit casein has a better blocking performance, it seems to mask the previous immobilized proteins, rendering them inaccessible. Conclusively, we employed BSA as blocking agent for subsequent experiments.

Since the PhyB/PIF interaction plays the key role in our experimental setup, we tested whether a competitor complex containing two PIF proteins shows better performance in terms of leakiness, i.e., fewer unspecific release during red-light illumination due to increased avidity. Therefore, the release of competitor complexes containing one or two PIF proteins was measured over a time range of 80 minutes. Additionally, to determine the unspecific release of the nitrocellulose membrane itself, the release of a biotinylated version of GFP-PIF6, immobilized directly on nAv, was determined. According to our findings (**Figure S3)**, the double PIF version has no advantages over the single version regarding the unspecific release (red light, 660 nm). In fact, the release of competitor molecules can be attributed to the unspecific release of the substrate itself as the biotin-GFP-PIF6 version shows similar values than the two other non-released samples. However, the specific release (far-red light, 740 nm) seems to achieve a higher release for the single PIF version, which is why we conducted all following experiments with this competitor version.

In order to find an assay architecture in terms of the assay area and their positioning, we tested three different variants regarding the diffusion time and fluid distribution on the distinct areas (**Figure S2**). For naked eye visualization, highly concentrated fluorescent protein mCherry (mCh) or a small molecule fluorescein was used. For both substances, the design variant where a small square shaped receiver area is enclosed by a larger square shaped sender area showed the best performance and was therefore employed for the following experiments

For the proof-of-principle assay, we first demonstrated the light-induced competition of analyte and competitor. To simulate and verify the competitive mode of the OptoAssay, three conditions were tested: (i) red light illumination without analyte where no release of the competitor is expected, (ii) far-red light illumination without analyte where a release but no competition of analyte and competitor is possible, and (iii) far-red light illumination with analyte, where both a release and competition are expected. The fluorescence intensity measurements of the nitrocellulose membranes after illumination show a strong decrease in fluorescence signal of the sender membranes illuminated with far-red light compared to those illuminated with red light. Far-red light illuminated samples without analyte display a slightly higher fluorescence than the ones where analyte was added (**Figure 2A**). This can also be confirmed by measuring fluorescence intensities of the membranes (**Figure 2B**). Also, the measurements of the supernatant collected (**Figure 1**confirm this observation as there is a lower fluorescence intensity for the with far-red illuminated samples without analyte than the samples with. When comparing the leakiness (i.e., unspecific release of competitor during red light illumination) to the red-light induced specific release by dividing the fluorescence intensity of the far-red by the red light illuminated sample, there is a 6.1-times increase in signals of the sample with analyte but only a 4.5-times signal increase for the sample without analyte. Since both samples were treated equally, except addition of an analyte protein, there is no obvious reason for those samples to behave differently. An explanation for this discrepancy might be a partial drying of the membrane after GFP-PIF6 addition and before illumination of the sample pair without analyte, which leads to PhyB denaturation and therefore, impairment of functionality. According to the fluorescence intensity of the receiver membranes, shown in **Figure 2C**, there was no negative effect on the competition itself; it is functional with even lower amounts of released competitor. While there is a high fluorescence intensity obtained from the sample treated with far-red light and without analyte, only a low fluorescence is detectable for the far-red light illuminated samples with analyte. A quantification of the fluorescence intensities of receiver membranes after illumination shows a 160% signal increase when comparing red light illuminated samples with far-red light illuminated ones without analyte and only a 20% increase in signals of far-red light illuminated membranes with analyte. This results in a

fluorescent signal increase of 120% when comparing far-red light illuminated samples with and without analyte.

The last step of the OptoAssay comprises of the rebinding of the unbound competitor molecules back to PhyB on the sender membrane which could enable a wash-free signal detection. To achieve this, one sample was illuminated first with far-red light to release the competitor and then with red light to rebind it. Control samples that were either illuminated with red or far-red light only were included as well. The fluorescence images of the membranes (**Figure 2D**) after illumination indicate that the control samples worked as anticipated. In the case of the sender membranes, the measured intensity of the far-red sample is lower than the red light one. Also, the binding of the competitor on the receiver membrane can be observed for the (far-red light illuminated) release samples (**Figure 2E**). The rebinding samples (illuminated with far-red and then red light) display a slight increase in fluorescence intensity of sender membranes. The rebinding of the unbound competitor was also demonstrated by measuring the supernatant fluorescence (**Figure 2F**) which corresponds the amount of free, unbound competitor. Here, the fluorescence intensity of the rebinding sample is only 0.6-times higher compared to the release sample. This means that about 40% of the released competitor could be rebound to the sender membrane. When comparing the membrane intensities (**Figure 2E**) before and after illumination, a reduction of fluorescence of the leakiness sample (red light) of 5% and 2% for sender and receiver, respectively, was observed. The release sample shows 36% reduction of intensity on the sender and a 23% increase on the receiver membrane. In the case of the rebinding sample, however, there is only a reduction of only 18% which indicates a partial rebinding. The receiver membranes prove only an increase of 7%. For this experiment, lower amounts of competitor were applied compared to the previous experiment to ensure a higher rebinding efficiency, as depicted in **Figure S3**. The general lower fluorescence intensity of the rebinding samples, however, could be attributed to the longer incubation time of 80 minutes compared with 40 minutes used for the other samples. The longer incubation period might have led to higher dissociation of PhyB and PIF6 or even the unspecific release of nAv from the nitrocellulose membrane (see **Figure S2**).

Having successfully demonstrated the proof-of-concept of the OptoAssay on a nitrocellulose substrate, we aimed to the test the general functionality of the optogenetic components on other substrates. As an alternative planar substrate, we used PMMA which is low-priced and thus, convenient for mass production of a potential POC device. A preliminary experiment (**Figure S5**) showed that nAv directly absorbs to untreated PMMA which circumvents the need for a surface functionalization. Subsequently, we immobilized biotinylated PhyB on the nAv coated surface. With this setup, we could demonstrate a spatially resolved release of the competitor complex from a PMMA substrate (**Figure S6**). However, we did not pursue with PMMA as a substrate because the total amount of immobilized photoreceptor was lower compared to nitrocellulose.

The next substrate tested were functionalized beads that are very often used as solid phase materials in bioassay applications in clinical and POC diagnostics[13,14]. In this setting, we verified the functionality of the optogenetic system on a bead-based platform where neutravidin (nAv) functionalized agarose beads are employed to immobilize the biotinylated PhyB. We simulated the reversibility of releasing and rebinding the PIF6 molecule as the competitor from PhyB as described in[9], immobilized on agarose beads (**Figure S7**). We could again show a light-dependent release as well as partial rebinding of competitor molecules from and to the substrate.

Conclusion and Outlook

Here, we have successfully demonstrated the proof-of-principle of an OptoAssay that enables, in contrast to conventional POC tests like LFAs, a bi-directional sample flow without any pump or flow control systems for a wash-free signal readout. Through a photoreceptor that can light-dependently interact with a binding partner, a competitor molecule can be released and later removed from the detection area by applying far-red and red light. Although other photoswitchable assays already exist[15,16], they only allow for detection of specific molecules, whereas the OptoAssay can be universally applied by fusing the molecule of interest to the phytochrome B interaction partner PIF6. For example,

the integrating of a z domain[17], an IgG-binding domain, antibodies can be attached to the PIF6 construct and act as detection antibodies to add even more versatility.

The system could also be further expanded by using or combining different optogenetic switches that respond to distinct wavelengths. For instance, the blue light receptor cryptochrome 2 (Cry2) that forms heterodimers with its interaction partner cryptochrome-interacting basic helix-loop-helix (CIB1), or another switch, light-induced dimer (iLID), which comprises of the blue light receptor light oxygen voltage 2 domain of avena sativa phototropin 1-SsrA (AsLOV2) and its binding partner stringent starvation protein b (SspB) could be employed[18]. However, both photoreceptors only enable an active associating with its interaction partner, the dissociation is a slow passive event induced by the absence of blue light. Therefore, the OptoAssay workflow might need to be adapted accordingly in order to use different photoreceptors.

Using a 3D printed PhotoBox along with a smartphone, the OptoAssay introduced can be employed for on-site applications. Herein, the PhotoBox could be extended by an excitation light and emission filter that allows for GFP detection using a smartphone. A low-cost and easy approach using paper-based filters in combination with a smartphone for a fluorescence readout has already been implemented[19]. Finally, automated sample illumination and evaluation of the results via a smartphone app could be realized for user friendly operation.

Another issue that must be addressed is the overall operation time of the OptoAssay which is, at the moment, mainly limited by diffusion of the biomolecules employed. Herein, there are two important factors: the overall distance the molecules have to travel between the two areas (*i.e.,* detection and immobilization zones) and the speed at which the molecules move. To decrease the distance, smaller assay areas could be designed and fabricated by micro/nanofabrication techniques. For increasing the speed, external energy, like ultrasonication, could be also applied to the system.

The OptoAssay provides the basics for a novel and dynamic bioassay format (independent of assay type and biomolecules employed, such as antibodies, proteins or nucleic acids) through its light

dependent two-way switch that can extend already existing POC devices and could pave the way for new classes of diagnostic devices in future, extending the capabilities of these state-of-the-art tools.

Acknowledgements

The authors would like to thank the Deutsche Forschungsgemeinschaft (DFG, German Research Foundation) for funding this work under grant number 404478562 and Germany's Excellence Strategy CIBSS - EXC-2189 - Project ID: 390939984. We would also like to thank Felicia Wieland for designing and building the PhotoBox.

Competing Interest

The authors declare no competing interests.

Contributions

C.D and W.W conceived the project. N.U., C.D., M.H designed, analysed, and interpreted experiments. N.U performed experiments. C.D and M.H supervised the project. N.U wrote the manuscript with support from all other authors.

References

1. Syedmoradi, L. & Gomez, F. A. Paper-based point-of-care testing in disease diagnostics. *Bioanalysis* **9**, 841–843 (2017).
2. Ding, X., Cheung, S. F., Cheng, S. K. L. & Kamei, D. T. Paper-Based Systems for Point-of-Care Biosensing. *J. Lab. Autom.* **20**, 316–333 (2015).
3. Dincer, C., Bruch, R., Kling, A., Dittrich, P. S. & Urban, G. A. Multiplexed Point-of-Care Testing – xPOCT. *Trends Biotechnol.* **35**, 728–742 (2017).
4. Dincer, C. *et al.* Disposable Sensors in Diagnostics, Food, and Environmental Monitoring. *Adv. Mater.* **31**, 1806739 (2019).
5. Ziegler, T. & Möglich, A. Photoreceptor engineering. *Front. Mol. Biosci.* **2**, 1–25 (2015).

6. Burgie, E. S. & Vierstra, R. D. Phytochromes: An atomic perspective on photoactivation and signaling. *Plant Cell* **26**, 568–4583 (2014).

7. Shimizu-Sato, S., Huq, E., Tepperman, J. M. & Quail, P. H. A light-switchable gene promoter system. *Nat. Biotechnol.* **20**, 1041–1044 (2002).

8. Levskaya, A., Weiner, O. D., Lim, W. A. & Voigt, C. A. Spatiotemporal control of cell signalling using a light-switchable protein interaction. *Nature* **461**, 997–1001 (2009).

9. Beyer, H. M. *et al.* Generic and reversible opto-trapping of biomolecules. *Acta Biomater.* **79**, 276–282 (2018).

10. Wieland, F. *et al.* Enhanced Protein Immobilization on Polymers — A Plasma Surface Activation Study. *Polymers (Basel).* **12**, 1–12 (2020).

11. Towbin, H., Staehelin, T. & Gordon, J. Electrophoretic transfer of proteins from polyacrylamide gels to nitrocellulose sheets: procedure and some applications. *Proc. Natl. Acad. Sci.* **76**, 4350–4354 (1979).

12. Hartmeier, W. *Immobilized Biocatalysts*. (Springer Berlin Heidelberg, 1988). doi:10.1007/978-3-642-73364-2.

13. Chou, J. *et al.* Porous Bead-Based Diagnostic Platforms: Bridging the Gaps in Healthcare. *Sensors* **12**, 15467–15499 (2012).

14. Qu, J., Chenier, M., Zhang, Y. & Xu, C. A Microflow Cytometry-Based Agglutination Immunoassay for Point-of-Care Quantitative Detection of SARS-CoV-2 IgM and IgG. *Micromachines* **12**, 433 (2021).

15. Horsley, J. R. *et al.* Photoswitchable peptide-based 'on-off' biosensor for electrochemical detection and control of protein-protein interactions. *Biosens. Bioelectron.* **118**, 188–194 (2018).

16. Adelizzi, B., Gielen, V., Le Saux, T., Dedecker, P. & Jullien, L. Quantitative Model for Reversibly Photoswitchable Sensors. *ACS Sensors* (2021) doi:10.1021/acssensors.0c02414.

17. Nilsson, B. *et al.* A synthetic IgG-binding domain based on staphylococcal protein a. *Protein Eng. Des. Sel.* **1**, 107–113 (1987).

18. Guntas, G. *et al.* Engineering an improved light-induced dimer (iLID) for controlling the localization and activity of signaling proteins. *Proc. Natl. Acad. Sci.* **112**, 112–117 (2015).

19. Ireta-Muñoz, L. A. & Morales-Narváez, E. Smartphone and Paper-Based Fluorescence Reader: A Do It Yourself Approach. *Biosensors* **10**, 60 (2020).

20. Gibson, D. G. *et al.* Enzymatic assembly of DNA molecules up to several hundred kilobases. *Nat. Methods* **6**, 343–345 (2009).

21. Beyer, H. M. *et al.* Synthetic Biology Makes Polymer Materials Count. *Adv. Mater.* **1800472**, 1800472 (2018).

22. Hörner, M., Yousefi, O. S., Schamel, W. & Weber, W. Production, Purification and Characterization of Recombinant Biotinylated Phytochrome B for Extracellular Optogenetics. *Bio-Protocol* **10**, 1–17 (2020).

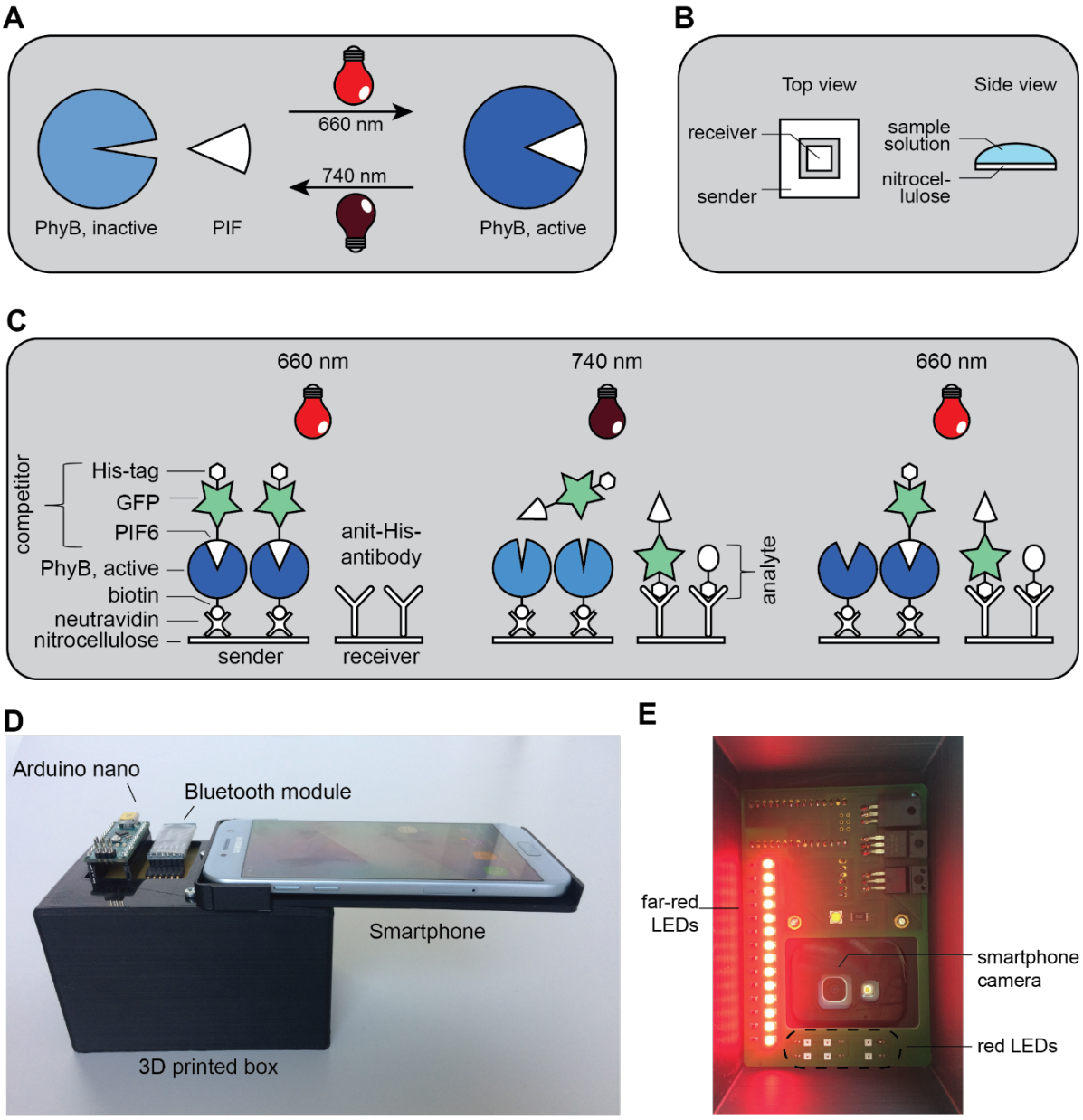

Figure 1. A) Scheme describing the basics of Phytochrome B (PhyB) and Phytochrome Interacting Factor (PIF) interaction. PhyB is transformed in the active form by illumination with red light (660 nm) where it interacts with PIF. By exposure to far-red light (740 nm), PhyB is converted to the inactive form where it cannot interact with PIF. **B)** Schematics describing the design of OptoAssay concept. The smaller square-shaped receiver area is enclosed by a larger square-shaped sender area. Both zones are connected with sample solution that covers them. **C)** Working principle of the OptoAssay. In the initial state, active PhyB is immobilized via nAv on the nitrocellulose sender area while the competitor complex (PIF6-GFP-his) is associated with PhyB during red light illumination. The receiver area is coated

with anti-his antibodies. In the second step, where the assay is illuminated with far-red light and the competitor is released from the inactive PhyB conformation while at the same time an analyte molecule (his-tagged protein) is added. Analyte and competitor compete now for binding to the antibody on the receiver area. The final step comprises of illumination with red light again in order to reassociate all unbound competitors to PhyB on the sender area. **D)** 3D printed PhotoBox that allows for sample illumination and signal readout for the envisioned POC scenario. A smartphone is placed on top of the box and connected via a Bluetooth module to an Arduino nano to switch on and off the illumination. Through a hole in the box, images can be taken with the smartphone camera. **E)** PhotoBox from inside: LEDs for far-red- and red-light illumination.

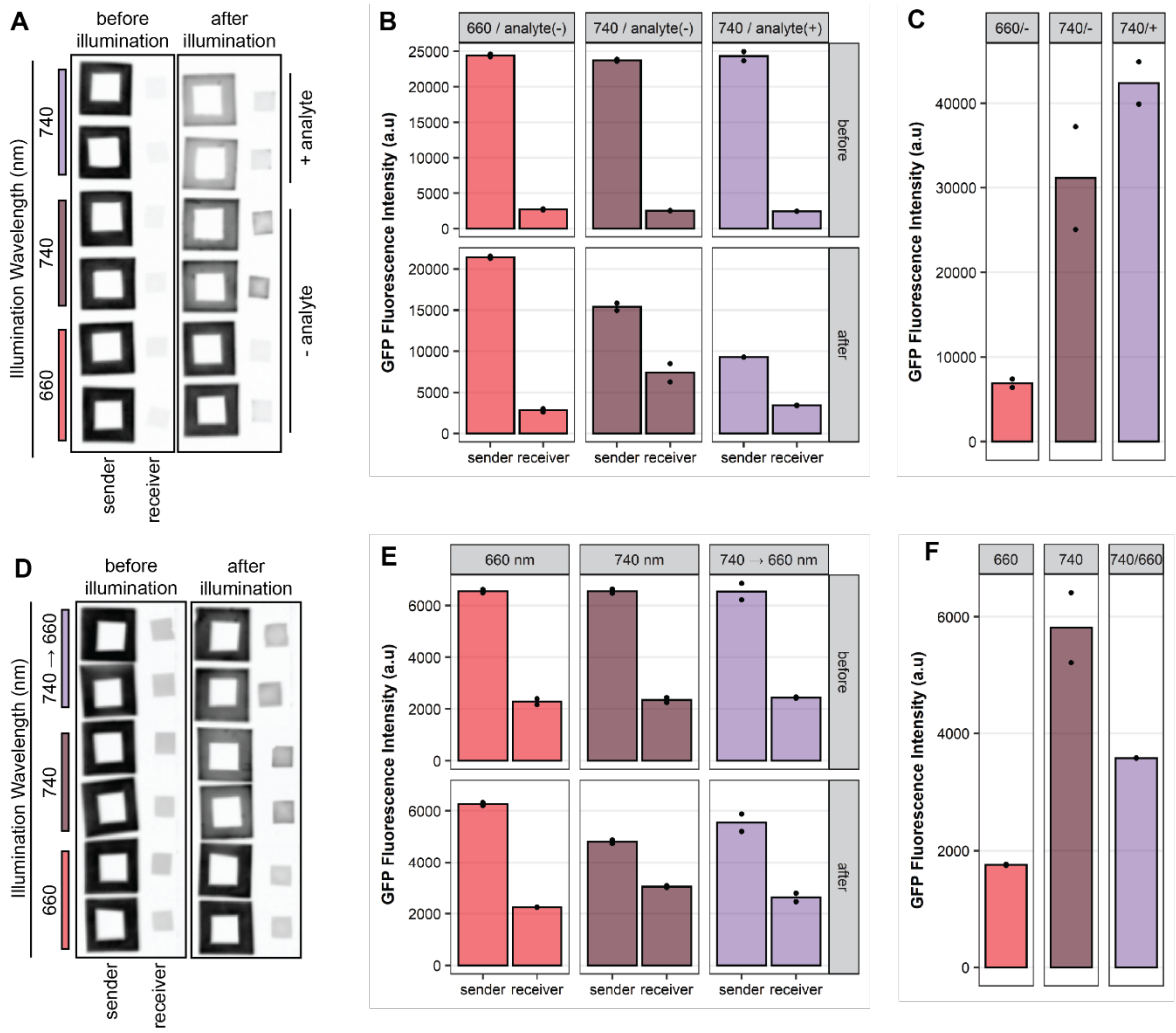

Figure 2. **A)** Release of the competitor and competition with an analyte on nitrocellulose membranes. Fluorescence images of nitrocellulose membranes before and after illumination. Sender membranes were incubated with nAv and then blocked with BSA. Later, biotinylated PhyB was immobilized. The competitor complex was bound to PhyB under red light illumination. The receiver membranes were coated with anti-his antibody and subsequently blocked with BSA. For the measurement, sender and receiver membranes were assembled and covered with buffer or buffer containing the his-tagged analyte protein which was added at the same time as illumination started. The samples were illuminated from above either with red or far-red light for 40 minutes. The membranes were washed under illumination with the corresponding light and subsequently stored in buffer until imaging. **B)** Membrane fluorescence intensity values measured from A in arbitrary units (a.u.) **C)** Supernatant fluorescence of the samples from A after illumination in a.u. **F)** Release and rebinding of the competitor

on nitrocellulose membranes. Fluorescence images of nitrocellulose samples before and after illumination. Sender membranes were incubated with nAv followed by blocking with BSA and immobilization of biotinylated PhyB. The competitor complex (his-GFP-PIF6, 1.3 µg ml^{-1}) was associated with PhyB under red light illumination. The receiver membranes were first coated with anti-his antibody (10 µg ml^{-1}) and subsequently blocked. Sender and receiver areas were assembled, and buffer was added to cover both areas. Illumination from above for 40 minutes either with red or far-red light or first 40 minutes with far-red and then 40 minutes with red light was carried out. Membranes were washed under illumination with the corresponding light and subsequently stored in buffer until imaging. **G)** Membrane fluorescence intensity values measured from Figure S4 in a.u. **H)** Supernatant fluorescence of the samples from E after illumination in a.u. Bars represent the mean of two replicates: red for red light illumination, dark red for far-red illumination, purple for first far-red and then red-light illumination. Single values are displayed as dots.

Methods

Plasmids and oligos

The DNA sequences of the plasmids generated and used in this study are shown in **Table 1** along with the templates and oligos for the polymerase chain reaction (PCR) to generate plasmids using Gibson cloning[20]. The sequences of the oligos used are listed in **Table 2**.

Table 1. Plasmids used for protein production. For plasmids cloned in this work, the templates (p) and corresponding primers (o) are listed below the construct.

Plasmid	Description	Reference	Used for
pHB111	Plac/T7-megfp-pif6(1-100)-H6	[21]	Figure 1D, 2B, 2E
pMH1105	Plac/T7-phyB(1-651)-GSGS-AviTag-H6, Plac/T7-ho-pcyA	[22]	All optogenetic experiments
pMH23	Plac/T7-zz-mcherry-pif6(1-100)-H6		Figure 1C
pKJ10	Plac/T7-H6-mcherry		Figure 1H
pMH1409	Plac/T7-zz-mcherry-pif6(1-100)-GSS-6xPAS-pif6(1-100)-H6 PAS-sequence:oMH1417/oMH1418 pMH023:oMH1419/oMH1420 pMH023:oMH1421/oHJW5 pMH023:oHJW6/oMH1422		Template for pMH1452
pMH1450	Plac/T7-zz-megfp-pif6(1-100)-H6 pHB111:oMH1500/oMH1501 pMH023:oMH1502/oHJW5 pMH023:oHJW6/oMH1503		Figure S3

pMH1451	Plac/T7-zz-megfp-pif6(1-100)-AviTag-H6 pHB111:oMH1500/oMH1501 pMH023:oMH1502/oMH1505 pMH023:oMH1504/oMH1503		Figure S3
pMH1452	Plac/T7-zz-megfp-pif6(1-100)-GSS-6xPAS-pif6(1-100)-H6 pHB111:oMH1500/oMH1501 pMH1409:oMH1502/oHJW5 pMH1409:oHJW6/oMH1503		Figure S3

Table 2. Primers used for PCR.

Oligo	DNA Sequence (5' → 3')
oMH1417	tggaaagcaataaacatgttgacggctcttctgcctctccagctg
oMH1418	ataatcggttggtaagaacatcatggcagcaggagcagacggg
oMH1419	gccccgtctgctcctgctgccatgatgttcttaccaaccgattattgttgcag
oMH1420	ttttaatggtgatggtgatgatggtcaacatgtttattgctttccaacatgtttgtttc
oMH1421	gttgaccatcatcaccatcaccattaaaag
oMH1422	gctggagaggcagaagagccgtcaacatgtttattgctttccaacatgtttg
oMH1501	catcataccagcagaacctgcggagcccttgtacagctcgtccatgcc
oMH1502	gcatggacgagctgtacaagggctccgcaggttctgc
oMH1503	tcctcgcccttgctcaccatgccagaaccgctacctgc
oMH1504	ggtctgaacgacatcttcgaagctcagaaaatcgaatggcacgaacatcatcaccatcaccattaaaagcttg

oMH1505	ttcgtgccattcgattttctgagcttcgaagatgtcgttcagaccgtcaacatgtttattgctttccaacatg
oHJW5	ctttgatcttttctacggggtctg
oHJW6	gcgtcagaccccgtagaaaag

Protein production and purification

PhyB constructs

PhyB-AviTag (pMH1105) bacterial pellets, stored at –80 °C, were dissolved in Ni-Lysis buffer 50 mM NaH_2PO_4, 300 mM NaCl, 10 mM imidazole, pH 8.0),10 ml buffer per 1 g bacterial pellet, for about 20 min at 4 °C by stirring. The suspension was lysed using a French press (APV 2000, APV Manufacturing) running three cycles at 1,000 bar. The lysate was centrifuged for 17,000 × g for 30 min at 4 °C, then the supernatant was transferred to a new vessel and centrifuged again for 30 min. After centrifugation, the supernatant was kept on ice until further processing. The protein was purified using a Ni-NTA Superflow column (Quiagen, Netherlands, 30761) on a Äkta Express fast protein liquid chromatography system (FPLC, GE Healthcare, USA). The lysate was loaded on the column which was afterwards washed with 12 column volumes Ni-wash buffer (50 mM NaH_2PO_4, 300 mM NaCl, 20 mM imidazole, 0.5 mM tris(2- carboxyethyl)phosphine (TCEP), pH 8.0). The protein was eluted in 6 column volumes Ni-elution buffer (50 mM NaH_2PO_4, 300 mM NaCl, 250 mM imidazole, pH 8.0). The eluted protein was stored at 4 °C or frozen at –80 °C. For freezing at –80 °C, the Ni elution buffer was replaced with DPBS Before exchanging the buffer, the purified protein was concentrated with concentration columns with a cut-off of 30 kDa (Corning Inc., USA, CLS431489). 100 mL of the purified protein were distributed into tow concentrator columns and centrifuging at 8,000 × g for 2 min, then the protein solution wax mixed by inverting; this process was repeated until a final volume of 4 mL. was reached. For the buffer exchange from Ni-elution buffer to DPBS a 10 mL dextran desalting column (ThermoFisher Scientific, USA, 1896121) was used. The protein was aliquoted, shock frozen in liquid nitrogen and stored at –80 °C.

PIF6 constructs

The proteins were produced in bacterial strains of E. coli BL21 (DE3) (Invitrogen, USA). Cells were harvested by centrifugation at 6,500 g for 10 min and resuspended in lysis and disrupted using a French Press at 1,000 bar or by sonication (Bandelin Sonopuls HD3100 (Bandelin, Germany), 12 min with 60% amplitude and 0.5 s/1 s pulses). Lysates were clarified by centrifugation at 30,000 g for 30 min and loaded on Ni^{2+}-NTA agarose columns (Qiagen, Netherlands). After washing with each 20 column volumes of lysis and wash buffer (50 mM NaH_2PO_4, 300 mM NaCl, 20 mM imidazole, pH 8.0), purified proteins were eluted in 5 column volumes of Ni elution buffer (50 mM NaH_2PO_4, 300 mM NaCl, 250 mM imidazole, pH 8.0). Finally, the proteins produced were quantified by fluorescence or by Bradford assay (Bio-Rad, USA).

Illumination Experiments

OptoAssay

For sender membrane preparation the nitrocellulose membranes were cut into squares (8 × 8 mm^2) and put into a 24-well plate. The squares were incubated with 300 µL nAv (1.5 mg ml^{-1} in DPBS) for 30 min. After washing with DPBS, the membranes were blocked with 300 µL BSA solution (5% in DPBS) for 1 h. Then, 300 µL of biotinylated PhyB (pMH1105, 1 mg mL^{-1} in DPBS) incubated for 30 min in the dark. After washing (0.1% BSA in DPBS), 300 µL of GFP-PIF6 (pHB111, 30mg mL^{-1} for competition and 1.5 µg mL^{-1} for rebinding in 5% BSA dissolved in DPBS) was incubated for 10 min under 660 nm illumination (30 s at 46 µmol m^{-2} s^{-1}, rest at 15 µmol m^{-2} s^{-1}) from above. The samples were afterwards washed again during 660 nm illumination.

Three sender area squares (3 × 3 mm^2) were put into a 24-well containing 300 µL of anti-His antibody (Merck, Germany, NOVG70796-3) (10 µg ml^{-1} in DPBS) and incubated for 30 min. The squares where then washed three times with 300 µL washing buffer (0.1% BSA in DPBS) followed by a blocking steps with 300 µL a BSA solution (5% BSA in DPBS) for 1 h. When using a biotinylated antibody (ThermoFisher

Scientific, USA, MA1-21315-BTIN) diluted in 5% BSA in DPBS, the membranes were first treated with 300 µL nAv (1.5 mg ml^{-1}) for 30 min. After washing, the membranes were blocked as previously described before adding the antibody solution.

For the experiment, the sender membranes were put onto a plastic plate covered with parafilm; the receiver membranes were put into the square opening of sender membranes. The plastic plate was put into a petri dish containing water to prevent evaporation. 80 µL of buffer (0.1% BSA in DPBS) was added to the assembled squares. For competition, 80 µL of a his-tagged protein pyruvate dehydrogenase complex repressor (pdhR) (0.3 mol L^{-1} in 0.1% BSA in DPBS) was used as analyte and was added at the same time as the illumination started. The samples were either illuminated with 660 nm (40 min at 15 µmol m^{-2} s^{-1}) or 740 nm (10 min at 380 µmol m^{-2} s^{-1}, 30 min at 200 µmol m^{-2} s^{-1}) from above. Before visualization, the samples were rinsed in beaker containing DPBS under illumination of the respective wavelength and put into new well containing DPBS. The GFP fluorescence of the nitrocellulose membranes was imaged using ImageQuant LAS 4000mini detector (GE Healthcare, USA). For fluorescence measurements of the supernatant, 50 µL of the supernatant was collected after removing the nitrocellulose membrane, and subsequently measured using a microtiter plate reader Tecan infinite M200pro (Tecan Group, Switzerland) (excitation wavelength: 488 nm, emission wavelength: 530 nm); background fluorescence of the buffer (0.1% BSA in DPBS) was subtracted from each value before plotting.

Total or spatially resolved release from nitrocellulose

Nitrocellulose membranes (ThermoFisher Scientific, USA, 88018) were cut into squares (8 × 8 mm^2) and put into a 24-well plate. The samples were incubated 300 µL nAv (1.5 mg ml^{-1} in DPBS) for 30 min. After with DPBS for 2 min, the membranes were blocked with 300 µL BSA solution (1% in DPBS) for 30 min if not stated otherwise. Then, 300 µL of biotinylated PhyB (pMH1105, 1 mg mL^{-1} in DPBS or Ni elution buffer) incubated for 30 min in the dark. After washing (0.1% BSA in DPBS), 300 µL of GFP-PIF6 (pMH1450, 3 × 10^{-2} mg mL^{-1} in 1 or 5% BSA dissolved in DPBS) was incubated for 30 min under 660 nm

illumination (46 µmol m^{-2} s^{-1}; 1 min on, 5 min off) from above. The samples were afterwards washed during 660 nm illumination.

For spatially resolved release with a photomask, samples were put directly on the photomask, covered with buffer (0.1% BSA in DPBS) and illuminated from below with 740 nm (77 µmol m^{-2} s^{-1}) light for 2 min. Immediately after illumination, the samples were rinsed in beaker containing DPBS and put into a new well containing DPBS. Experiments without a photo mask were conducted in a 24-well plate, where a volume of 300 µL buffer was added before 740 nm (380 µmol m^{-2} s^{-1}) or 660 nm (46 µmol m^{-2} s^{-1}). Supernatant samples of 50 µL were taken at the indicated timepoints. Before visualization, the samples were rinsed in beaker containing DPBS under illumination of the respective wavelength and put into new well containing DPBS.

For testing the different PIF6 versions, GFP-PIF6 (pMH1450) and GFP-2xPIF6 (pMH1452), the nitrocellulose membranes where prepared as previously described. For the samples treated with biotin-GFP-PIF6, the PIF construct was added directly to nAv functionalized and blocked membranes; this sample was only illuminated with red-light. Fractions of the supernatant (50 µL) of all samples were taken at five time-points during the 80-minute illumination period. The samples were measured using a plate-reader (excitation wavelength: 488 nm, emission wavelength: 530 nm); background fluorescence of the buffer (0.1% BSA in DPBS) was subtracted from each value before plotting. The GFP fluorescence of the nitrocellulose membranes was measured using ImageQuant LAS 4000mini detector.

Agarose Beads

For ten samples, 100 µL nAv functionalized agarose beads (ThermoFisher Scientific, USA, 29202), corresponding to 200 µL slurry, were washed with buffer (0.1% (w/v) BSA in DPBS) by centrifugation at 8,000 × g for 2 min. Then 800 µL PhyB (pMH1105, 2 mg mL^{-1} in Ni elution buffer) was added and incubated for 30 min in the dark. PhyB solution was removed, and the samples were washed. 600 µL of mCh-PIF6 (pMH23, 2.9 or 0.029 mg ml^{-1} in 0.1% BSA in DPBS) were added and incubated for 30 min

under 660 nm illumination (46 µmol m^{-2} s^{-1}; 1 min on, 5 min off). After washing, the beads were re-suspended in 2 mL buffer (0.1% BSA in DPBS). For each sample, 200 µL of the re-suspended beads were transferred into a 1.5 mL reaction tube.

The reaction tubes were put on the bottom of an illumination box and were illuminated for 1 h at 660 nm (15 µmol m^{-2} s^{-1}) or at 740 nm (380 µmol m^{-2} s^{-1}) from above. After illumination, the samples were spun down at 8,000 × g for 2 min and 50 µL of the supernatant was taken for fluorescence measurements. The mCh fluorescence (excitation wavelength: 587 nm, emission wavelength: 625 nm) of the supernatant was detected using a microtiter plate-reader Tecan infinite M200pro; the background signal of the buffer was subtracted from each value before plotting.

Spatially resolved release from PMMA

PMMA (Röhm GmbH, Germany, 99524 GT, 1.175 mm) rectangles (2 × 1.5 cm^2) were cut and put into a 6-well plate. The samples were incubated with 1 mL of nAv (ThermoFisher Scientific, USA, 31050) solution (1.5 mg ml^{-1} in DPBS) for 30 min. After washing with buffer (0.1% BSA in DPBS) for 2 min followed before incubating PhyB (pMH1105, 2 mg mL^{-1} in Ni elution buffer) for 30 min in the dark. After washing, 1 mL of GFP-PIF6 (pMH1450, 1 mg ml^{-1} in Ni elution buffer) was incubated under 660 nm (46 µmol m^{-2} s^{-1}; 1 min on, 5 min off) illumination. The samples were afterwards washed again. Samples were put directly on the photomask, covered with buffer (0.1% BSA in DPBS) and illuminated from below with 740 nm (77 µmol m^{-2} s^{-1}) for 1 min. Immediately after illumination, the samples were rinsed in beaker containing DPBS and put into a new well containing DPBS. For visualization, the GFP fluorescence of the PMMA slides were imaged using ImageQuant LAS 4000mini detector.

Assay Design Diffusion experiment

Cellulose sender areas were incubated in solution of a fluorescent protein mCh (molecular weight: 27,545 g mol^{-1}, concentration: 0.2 mM) or fluorescein (molecular weight: 332 g mol^{-1}, concentration: 10 mM) for 10 minutes. The treated sender and the untreated receiver membrane were assembled. Sender and receiver membranes were covered with DPBS, then images of the membranes were taken immediately after assembly and after 5, 10, 15, and 30 minutes.

PhotoBox with integrated electronics

The 3D printed PhotoBox serves as incubation unit by illumination with 660 nm (12 µmol m^{-2} s^{-1}) and 740 nm (185 µmol m^{-2} s^{-1}) light and as imaging box with a smartphone-based readout. For smartphone, a Samsung Galaxy A5 (2017) (Samsung Electronics, South Korea) is used. The images are taken during flashlight illumination with the integrated smartphone camera. The LEDs can be switched on and off via an Arduino nano, which receives the signal via an HC-05 Bluetooth module. The Arduino nano is coded, so that the user only needs to send either "660 nm" or "740 nm" via smartphone to the HC-05 in order to turn on/off the LEDs. Here, a standard application for Android is used as Bluetooth terminal to connect to HC-05.

The PhotoBox was designed with SolidWorks 2014 (Dassault Systemes SolidWorks Corp., France) and printed out of black acrylonitrile butadiene styrene (ABS) with the Ultimaker 3 (Ultimaker B.V., Netherlands). The PCB was designed with EAGLE software and produced by the company Beta LAYOUT Ltd. (Germany) and the soldering of the electronic components was done in-house.

Data analysis

For analysis of the GFP fluorescence intensity on nitrocellulose/PMMA, an ImageQuant LAS 4000mini detector (GE Healthcare, USA) was employed. The images were analyzed using the software ImageJ (University of Wisconsin-Madison, USA). The intensity of the whole nitrocellulose membranes/PMMA

pieces or the illuminated and not illuminated areas were analyzed with the area selection tool. In order to determine the final value of intensity, the background intensity was subtracted, and the obtained values were normalized.

For analysis of the fluorescence intensity in the supernatant, the fluorescence of mCh (excitation wavelength: 587 nm, emission wavelength: 625 nm) or GFP (excitation wavelength: 488 nm, emission wavelength: 530 nm) was measured with a Tecan infinite M200pro (Tecan Group, Switzerland) plate-reader. For normalization, intensity values of plain buffer were subtracted from each value.

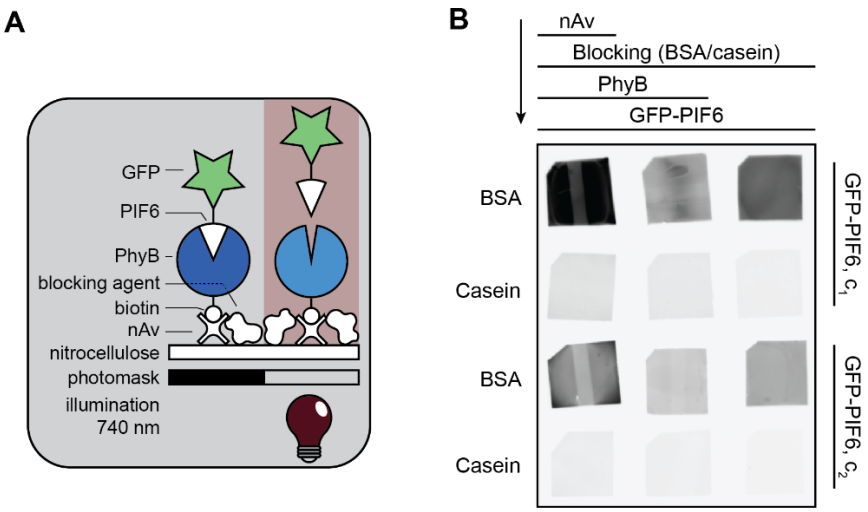

Figure S1. Blocking Strategy. A) Experimental setup. The nitrocellulose membrane was incubated with nAv, then blocked with a blocking agent (BSA or casein). Finally, GFP-PIF6 was immobilized. **B)** Comparison of blocking efficiencies using BSA or casein. Image of nitrocellulose membranes before addition GFP-PIF6. All membranes were incubated with nAv, then blocked with 5% BSA or 1% casein. Biotinylated PhyB was incubated on the nAv functionalized membranes. The image was taken after washing away unbound PhyB. **C)** GFP fluorescence of nitrocellulose membranes after the addition of GFP-PIF6 and illumination with far-red light (740 nm) through a photomask for 2 min. The samples from **A)** were incubated with two different concentrations of GFP-PIF6 ($c_1 = 3 \times 10^{-2}$ mg mL^{-1} and $c_2 = 0.6 \times 10^{-2}$ mg mL^{-1}) during red light illumination (660 nm). The samples were covered with buffer before illumination with far-red light through a photomask.

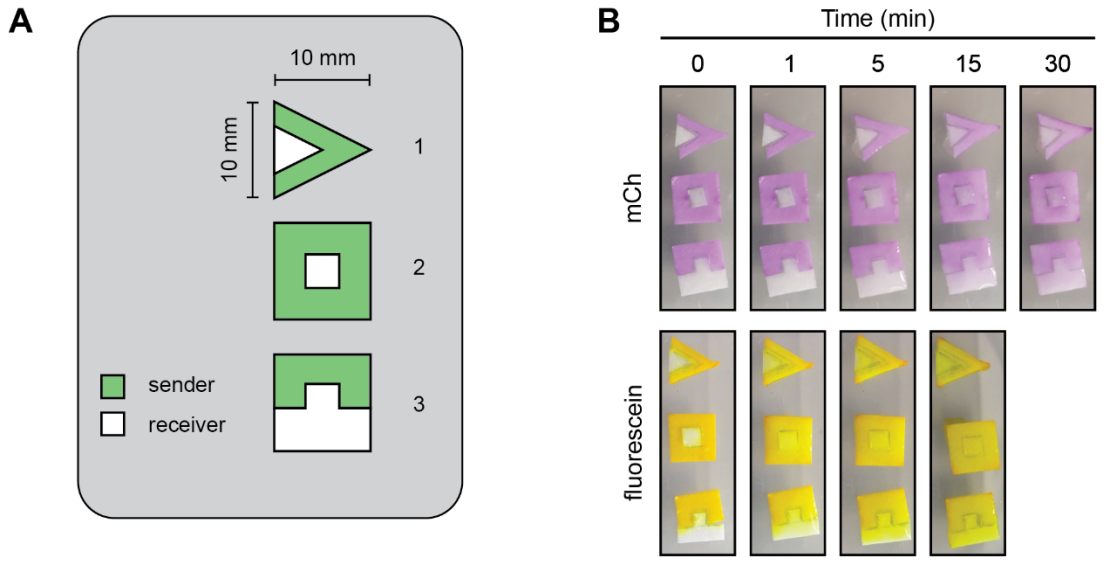

Figure S2. Geometry of OptoAssay Areas. A) Design of sender and receiver area. Sketch of different design variants. **B)** Images of the diffusion measurement from sender to receiver membrane. Cellulose sender areas were incubated in solution of a fluorescent protein mCherry (mCh) the small molecule fluorescein. The treated sender and the untreated receiver membrane were assembled and covered with buffer. Images were taken immediately after assembly and after 5, 10, 15, and 30 minutes.

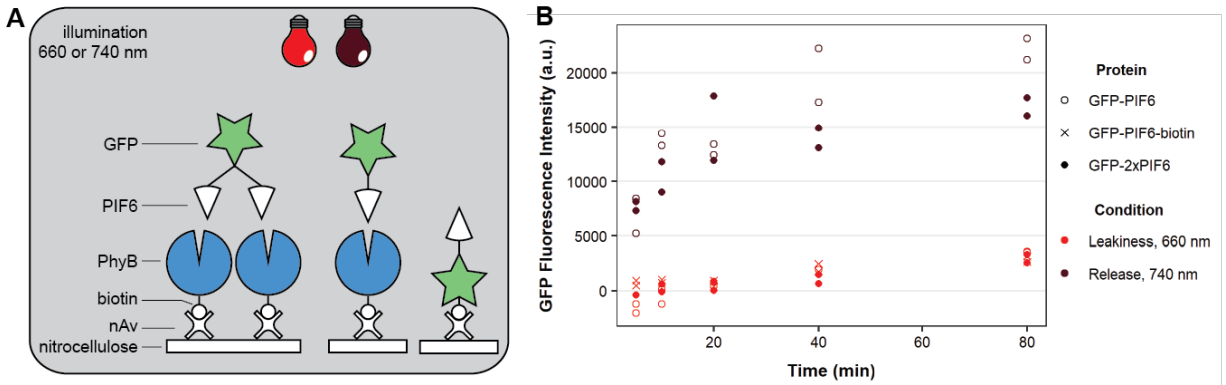

Figure S3. Different PIF6 Versions. A) Experimental setup. nAv treated nitrocellulose membranes were either incubated with PhyB before addition of GFP-PIF6 or GFP-2xPIF6. GFP-PIF6-biotin was directly immobilized on the nAv-coated membranes. **B)** Release kinetics of the model cargo GFP from functionalized nitrocellulose. nAv was immobilized on nitrocellulose before BSA-blocking. Biotinylated PhyB was subsequently added to the samples; except for the sample treated with GFP-PIF6-biotin. The

different cargo proteins GFP-PIF6, GFP-PIF6-biotin or GFP-2xPIF6 (3×10^{-2} mg mL^{-1}) were incubated during red light illumination. The samples were illuminated from above in a 24-well plate, covered with buffer, for 80 min either with red (660 nm; 5 µmol m^{-2} s^{-1}) or far-red light (740 nm; 380 µmol m^{-2} s^{-1}). Graph shows the GFP fluorescence of supernatant over a time range of 80 min in a.u. 50 µL of the supernatant at timepoints 5, 10, 40 and 80 min were taken for GFP fluorescence measurements. The background fluorescence of the buffer was subtracted from each value. Lines display the mean of two replicates, dots the single values. Red markings represent samples illuminated with 660 nm, while dark-red ones the samples illuminated with 740 nm.

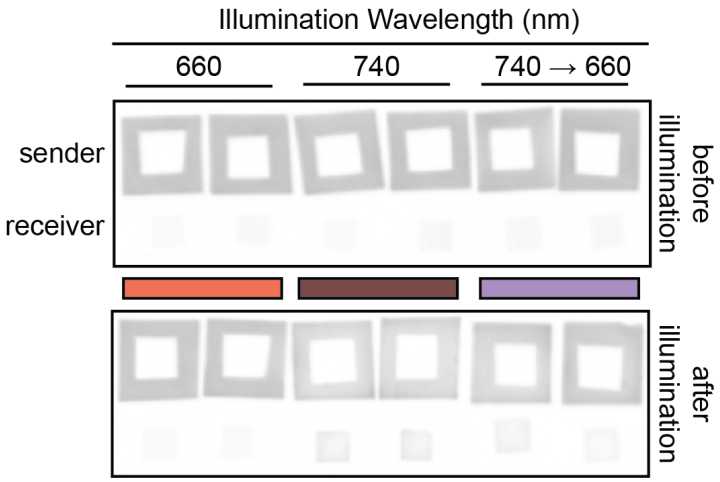

Figure S4. Original Membrane Intensities. Membrane intensities of Figure 2E with the same contrast settings as Figure 2B.

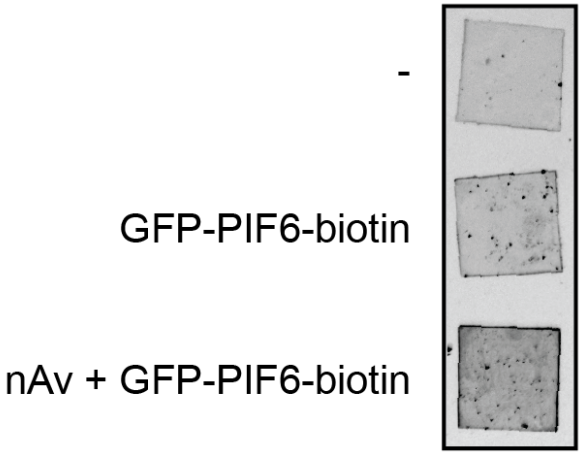

Figure S5. Adsorption Test on PMMA Samples. GFP fluorescence images of PMMA samples. PMMA slides were either incubated in PBS (-), or GFP-PIF6-biotin was added directly. For the sample containing nAv, the PMMA substrate was blocked with 5% BSA after nAv incubation. Then GFP-PIF6-bition was added. The images were taken after washing the samples.

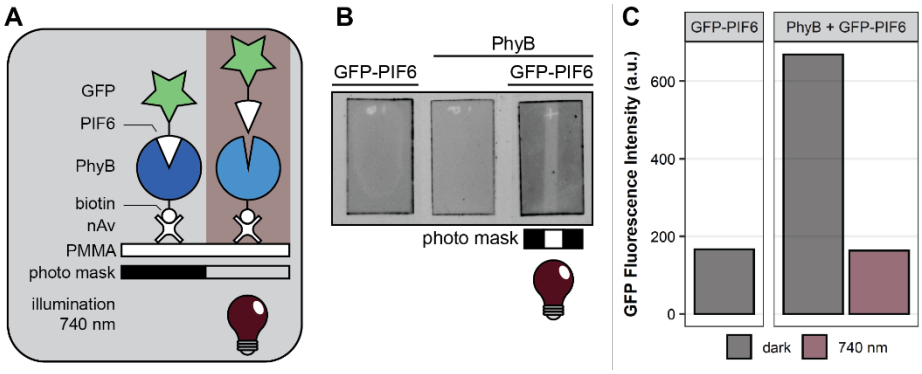

Figure S6. Release Experiments on PMMA Substrate. A) Experimental setup of the spatially resolved release of the competitor complex PIF6-GFP from PMMA. Competitor complex was immobilized via biotinylated PhyB on PMMA treated with neutravidin (nAv). The samples were illuminated from below with far-red light (740 nm) through a photomask. **B)** GFP fluorescence images of PMMA samples. First nAv was adsorbed on PMMA, then biotinylated PhyB was added to the indicated samples. After blocking, GFP-PIF6 was incubated on the indicated samples during red light (660 nm) illumination. Two samples were either treated with only biotinylated PhyB or GFP-PIF6 after blocking. The PMMA sample containing both PhyB and PIF6 was then put on a photomask and after addition of buffer to cover the

whole area, the sample was illuminated through photomask with far-red light (740 nm) from below for 1 min. The other samples were left in the dark. **C)** Quantification of fluorescence intensity measured from B in a.u. The background fluorescence of the PhyB only sample was subtracted from all samples before plotting. Black bars display the intensity of the not-illuminated samples/areas; the dark-red bar displays the intensity of the illuminated area.

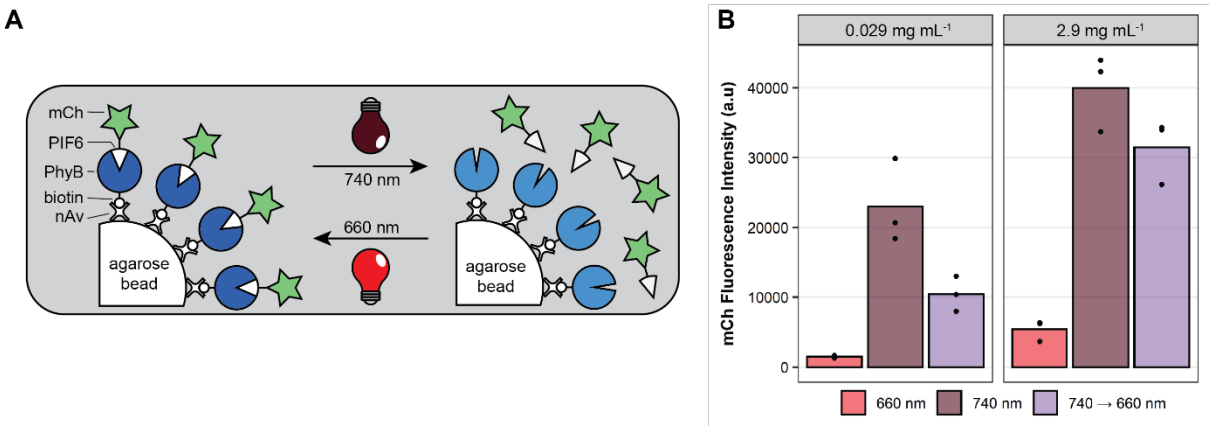

Figure S7. Release and Rebinding Experiments on Beads. A) Experimental setup of release and rebinding of the competitor complex PIF6-mCh from and to nAv functionalized agarose beads. Illumination with far-red light (740 nm) leads to a release of competitor from PhyB; during red light (660 nm) illumination mCh-PIF6 and PhyB are associated. **B)** For the preparation, 10 µl PhyB coated beads were incubated with two different concentrations of mCh-PIF6 (0.029 or 2.9 mg ml^{-1}) under red light illumination. For this experiment, the loaded beads were incubated in buffer and either illuminated with red or far-red light for 1 h or first with far-red light for 30 min and then with red light for 30 min. The mCh fluorescence intensity was measured in a.u. from the supernatant of the sedimented beads. The background fluorescence of the buffer was subtracted from each value. The means of 3 replicates (dots) are displayed as bars.